Supplementary information

Nitrogen and Phosphorus Enriched Inorganic-Organic Hybrid Material for Electrochemical Detection of Selenium(IV) Ions

*Arun Kumar[ψ], Prakriti Thakur[ψ], Nisha Dhiman, Sachin Balhara, and Paritosh Mohanty**

Functional Materials Laboratory, Department of Chemistry, Indian Institute of Technology (IIT) Roorkee, Roorkee, Uttarakhand-247667, India

[*]Email: paritosh75@gmail.com, pm@cy.iitr.ac.in

[ψ]Both authors have equal contribution

1. Experimental details

1.1. Synthesis of HPHM

The synthesis of HPHM was carried out as per our previous report [S1]. In the standard preparation of HPHM, 6 mmol (0.65 g) of DAP was dissolved in 10 mL of anhydrous DMSO in a Schlenk flask. A solution containing 1 mmol (0.35 g) of PNC (99% Sigma Aldrich, UK), dissolved in 10 mL of dry DMSO, was added gradually to the above solution under an argon atmosphere at 140 °C. The reaction mixture was then stirred for 18 hours. A product with a deep green color was acquired, which was filtered and rinsed with deionized water. The product was then dried at 80 °C for 12 h.

1.2. Material characterization

Fourier transform-infrared (FT-IR) (Spectrum Two, PerkinElmer) spectroscopy was employed to characterize the structure of the synthesized material (HPHM). FT-IR spectra were recorded using a KBr pellet in the range of 400 to 4000 cm^{-1}. Furthermore, Wide-angle powder X-ray diffraction (XRD) analysis was carried out (XRD; Ultima IV; Rigaku) using Cu Kα radiation (λ = 1.5405 Å). The XRD data were obtained over a 2θ range of 10 to 80 degrees at a scanning

speed of 5° min^{-1}. The textural properties were evaluated by using Autosorb iQ2 (Quantachrome Instruments, USA). The specimens were prepared for analysis by outgassing at 150 °C for five hours under vacuum conditions. Following this, the N_2 sorption isotherm was measured at a temperature of -196 °C and a pressure of 1 bar. The BET model was used to evaluate the specific surface area (SA_{BET}) within the pressure range of 0.05 to 0.30 (P/P_0). The pore size distribution (PSD) was determined using the Density Functional Theory (DFT) method with the Kernel "N_2 at 77 K on carbon: Slit Pores, QSDFT equilibrium model." Additionally, the pore volume was obtained at a relative pressure of P/P_0 of 0.99. The FESEM image of the HPHM was recorded on Zeiss Ultra Plus (Carl Zeiss) with an operating voltage of 20kV. The TEM images were obtained using TECNAIG2S-TWIN microscope.

1.3. Electrochemical characterizations:

The anodic and cathodic peak current was increased linearly with the square root of scan rates ($v^{1/2}$) from 5 to 100 mV s^{-1}, which could be represented by the Randle-Sevick equation [S2] :

$$i = (2.69 \times 10^5) \times n^{\frac{3}{2}} \times A \times C \times D^{\frac{1}{2}} v^{\frac{1}{2}} \qquad (s1)$$

Where, i = the anodic and cathodic peak current,

n = the number of transferred electrons,

A = electrode surface area (cm^2)

C = concentration of the electroactive species (mol L^{-1}),

D = diffusion coefficient of $[Fe(CN)_6]^{3-/4-}$ (6.70×10^{-7} cm^2 s^{-1}) and

v = scan rates (V s^{-1})

After modifying the Randle-Sevick equation:

$$\frac{i}{v^{1/2}} = (2.69 \times 10^5) \times n^{\frac{3}{2}} \times A \times C \times D^{\frac{1}{2}} \qquad (s2)$$

Where, $\frac{i}{v^{1/2}}$ is the slope of the i_p linear fitting equation, the n is number of electrons is 1 for $[Fe(CN)_6]^{4-} \rightleftharpoons [Fe(CN)_6]^{3-} + e^-$. The above equation was used to calculate the electrochemical active surface area of the electrode material.

The diffusion coefficient is calculated by EIS using the following equation:

$$D = 0.5\left(\frac{266.11}{\sigma_\omega \times C}\right)^2 \times 10^{-12} \qquad (s3)$$

Where D is diffusion coefficient in $cm^2\ s^{-1}$, σ_ω is Warburg coefficient, C is the concentration in molar (mol cm^{-3}).

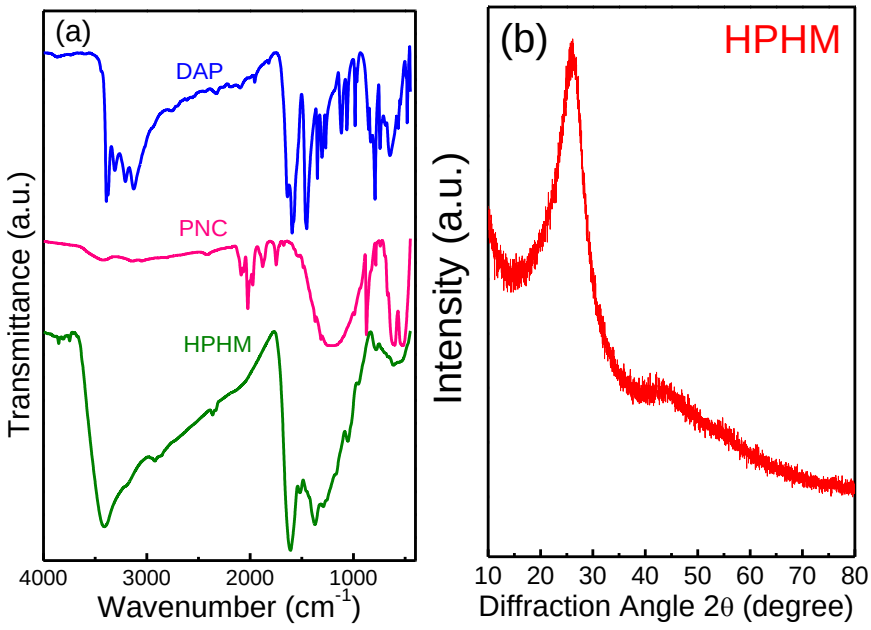

Fig. S1. (a) FT-IR spectra of DAP, PNC and HPHM and (b) XRD pattern of HPHM.

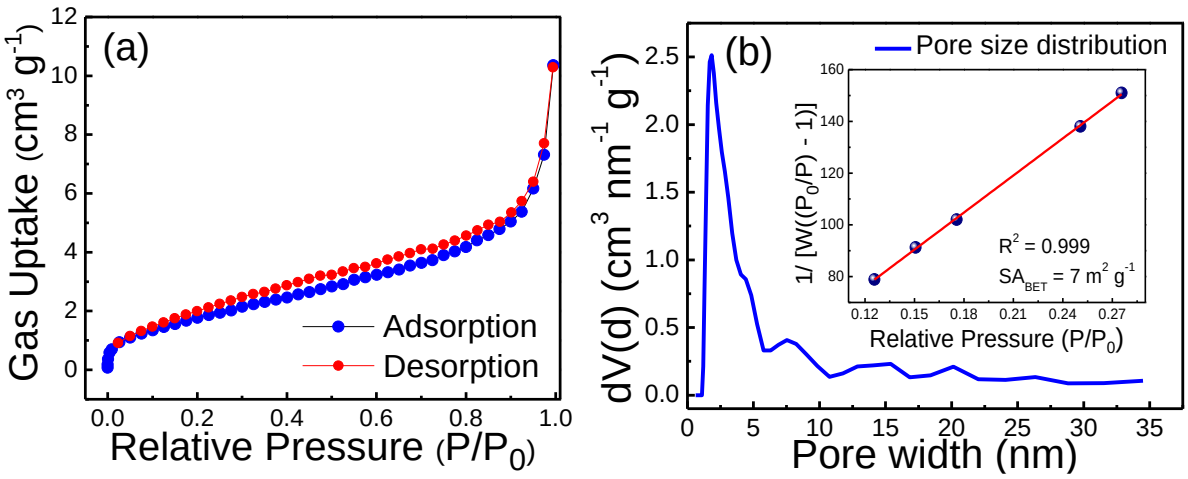

Fig. S2. (a) N_2 sorption isotherm of HPHM, and (b) pore size distribution (PSD) (inset: Multipoint BET plot) of HPHM.

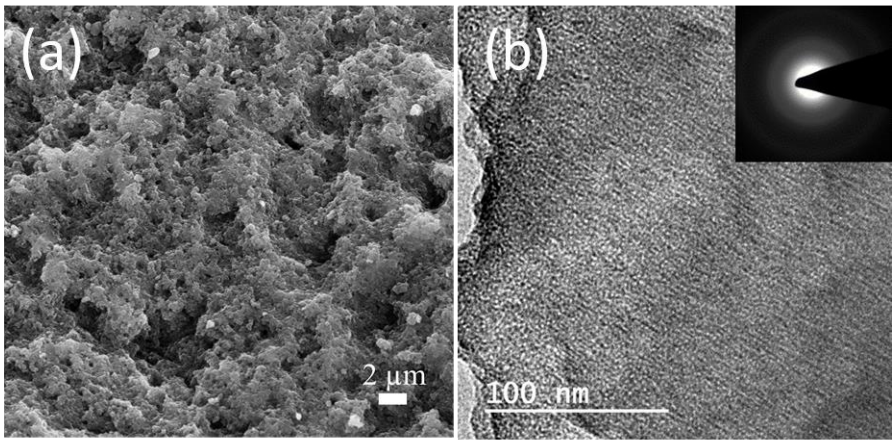

Fig. S3. (a) FESEM and (b) TEM (inset: SAED pattern) images of HPHM.

Table S1. Current response vs active mass loading of HPHM towards Se(IV) ions.

S. No	Active mass loading (mg)	Current at the peak (mA)
1	2.2	0.45
2	2.9	0.51
3	3.6	0.55
4	4.1	0.62
5	4.5	0.50
6	5.1	0.41

Table S2. Current response vs deposition time for HPHM towards Se(IV) ions.

S. No	Deposition time (s)	Current at the peak (mA)
1	80	0.54
2	110	0.55
3	140	0.56
4	170	0.60
5	200	0.59
6	230	0.57

Table S3. Current response vs deposition potential for HPHM towards Se(IV) ions.

S. No	Deposition potential (V)	Current at the peak (mA)
1	-0.8	0.57
2	-1.0	0.58
3	-1.2	0.63
4	-1.4	0.59
5	-1.6	0.58

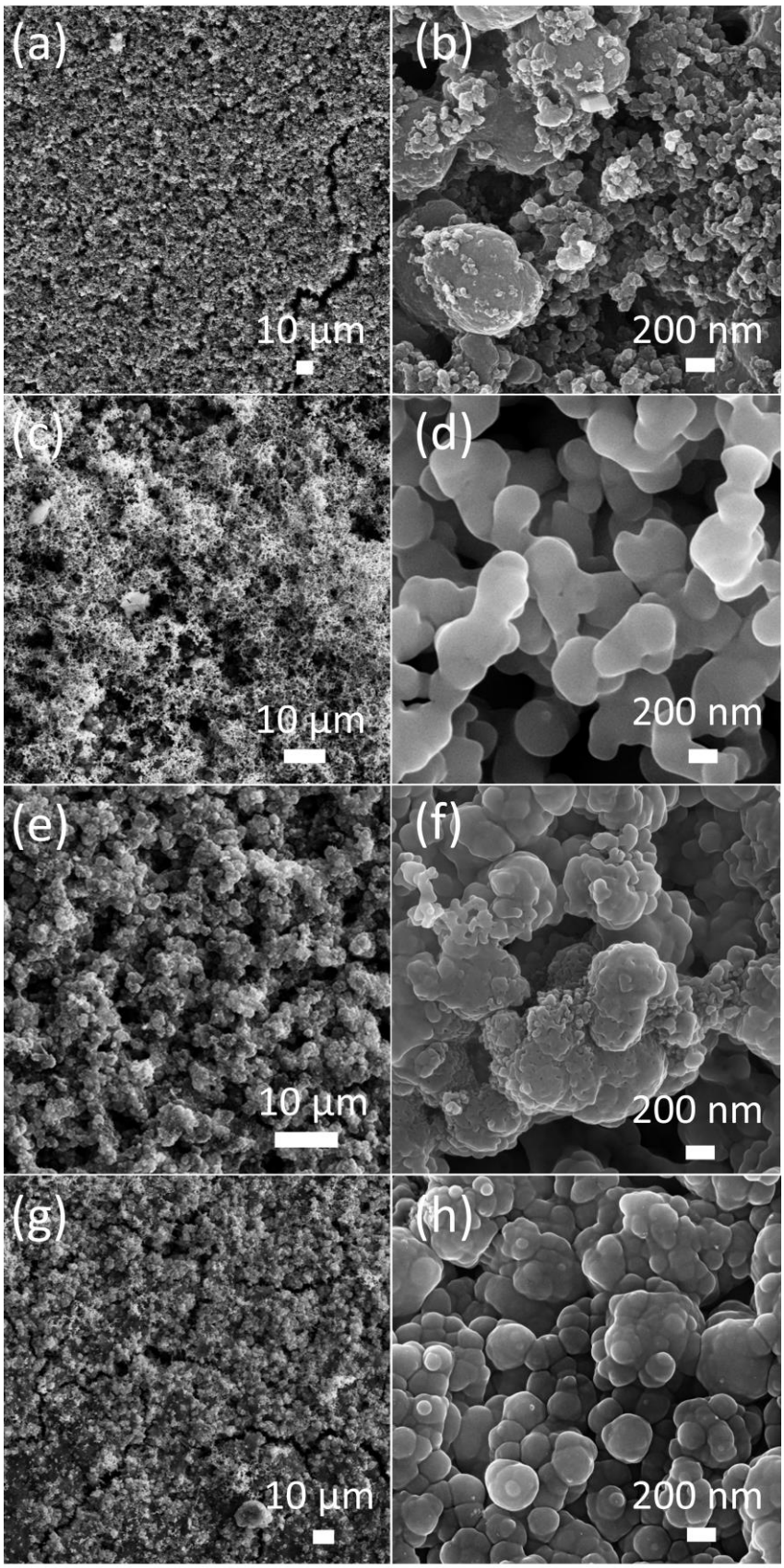

Fig. S4. FESEM image of (a-b) prinstine electrode (before used), (c-d) after DT of 200 s , (e-f) after DP -1.4 V, and (g-h) after 200 cycles at optimized conditions.

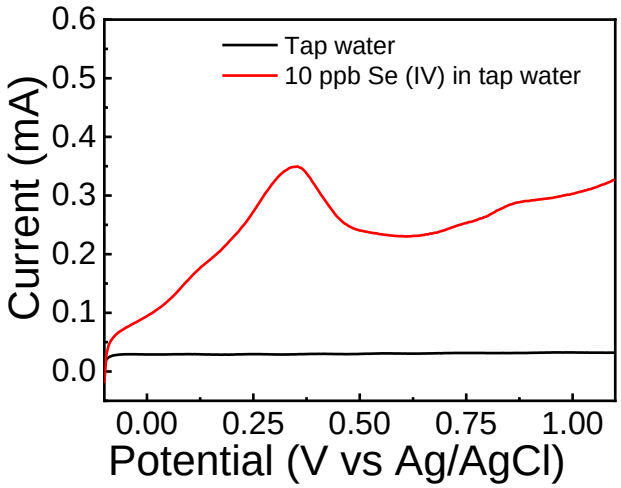

Fig. S5. DPV of tap water and 10 ppb solution of Se(IV) in tap water.

Table S4. Selected studies on the determination of inorganic selenium in water.

S.N.	Electrode	Methods	Potential Profile		Analytical Details		Ref.
			Deposition potential (DP) (V)	Deposition time (DT) (s)	LOD (ppb)	LR (ppb)	
1	HMDE	LSCSV	-0.35	180	4.73	-	S3
2	HMDE	DPCSV	-1.05	270	16.23	-	S4
3	Fe-Impregnated biochar from food waste	-	-	-	3.2	-	S5
4	MFE/Ag	DPCSV	-0.25	45	17	0.04-8	S6
5	Au/BDD	ASV	-0.4	120	10	10-100	S7
6	Graphite SPEs	ASV	-0.6	300	4.9	10-1000	S8
7	Screen print graphite electrode	-	-	-	19.2	10-1000	S9
8	Gold, modified Boron doped diamond electrode	-	-	-	20	-	S10
9	SiO_2 (NPs) grafted with 3-(2-aminoethylamino) propyltrimethoxysilane	-	-	-	11.33	15-100	S11
10	Au/ZnO/ITO	SWASV	0.6 V	-	2.89	5-100	S12
11	HPHM fabricated on graphite sheet	DPV	-1.2 V	170	2.18	5-50	This work

LSCSV: ; DPCSV: Differential pulse cathodic stripping voltammetry; ASV: Anodic stripping voltammetry; SWASV: Square wave anodic stripping voltammetry; DPV: Differential pulse voltammetry; LOD: Limit of detection; LR: Linear range.

Reference

[S1] N. Dhiman, P. Mohanty, *New J. Chem*., 2019, **43**, 16670-16675.

[S2] A. J. Bard, L. R. Faulkner, Electrochemical Methods: Fundamentals and Applications, (2000), 2nd edition. Wiley Global Education.

[S3] G. Mattsson, L. Nyholm, Å. Olin, *J. Electroanal. Chem*., 1994, **379**, 49-61.

[S4] C. Locatelli, G. Torsi, *J. Electroanal. Chem*., 2001, **509**, 80-89.

[S5] S. -H. Hong, F. N. Lyonga, J.-Kyu, Kang, E. -J. Seo, C. -G. Lee, S. Jeong, S. -G. Hong, S. -J. Park, *Chemosphere*, 2020, **252**, 126475.

[S6] T. B. Rubinskaya, S. V. Kovaleva, E. M. Kulagen, V. P. Gladyshve, *J. Anal. Chem*., 2003, **58**, 165-170.

[S7] C. F. Pereira, F. B. Gonzaga, A. M. Guarita-Santos, J. R. SouzaDe, *Talanta*, 2006, **69**, 877-881.

[S8] N. Y. Stozhko, E. I. Morosanova, L. I. Kolyadina, S. V. Fomina, J. Anal. Chem., 2006, **61**, 158-165.

[S9] A. V. Kolliopoulos, J. P. Metters, C. E. Banks, *Anal. Methods*, 2013, **5**, 851-856.

[S10] T. A. Ivandini, Y. Einaga, *Electrocatalysis*, 2013, **4**, 36-374.

[S11] C. Shi, G. S. Ding, A. N. Tang, Y. Y. Qiao, *Anal. Methods*, 2017, **9**, 1658-1664.

[S12] R. Jain, A. Thakur, P. Kumar, J. Pooja, *Electrochim. Acta*, 2018, **290**, 291-302.